



Full paper / Mémoire

A nanoscale study of the adhesive contact

Maurice Brogly *, Olivier Noel, Houssein Awada, Gilles Castelein, Jacques Schultz

Institut de chimie des surfaces et interfaces, (ICSI)–CNRS UPR 9069, université de haute Alsace (UHA), 15, rue Jean-Starky, 68057 Mulhouse cedex, France

Received 9 February 2005; accepted after revision 31 August 2005

Available online 22 December 2005

Abstract

Analysis of adhesive and mechanical properties of model polymer surfaces can be achieved with an Atomic-Force Microscope (AFM), in contact mode. The purpose of this study is to dissociate the different contributions (chemical and mechanical) included in an AFM force-distance curve in order to establish relationships between interfacial tip-polymer interactions and surface viscoelastic properties of the polymer. Surface force measurements are, in a first step, done on chemically modified silicon substrates (grafted with hydroxyl, amine, methyl and ester functional groups). In order to investigate the effects of mechanical or viscoelastic contributions, force measurements on model polydimethylsiloxane (PDMS) networks, whose surfaces are chemically modified with the same functional groups as for silicon substrates, were achieved. New relationships are proposed between the local adhesion force and both the dissipation energy in the tip-polymer contact and the surface properties of the materials (thermodynamic work of adhesion). Moreover the dissipation function is related to M_c , the mass between crosslinks of the polymer network. **To cite this article:** M. Brogly et al., C. R. Chimie 9 (2006).

© 2005 Académie des sciences. Published by Elsevier SAS. All rights reserved.

Résumé

La microscopie à force atomique offre, par l'intermédiaire d'une sonde de taille nanométrique, le moyen d'analyser mécaniquement les propriétés locales de surface des systèmes polymères, déterminantes quant aux propriétés finales de multimatériaux polymères. Dans un premier temps, les impératifs expérimentaux qui permettent l'obtention de mesures quantitatives sont exposés. La seconde partie du manuscrit traite de l'étude de systèmes modèles de chimie de surface contrôlée. Ce contrôle est réalisé par greffage chimique de silanes fonctionnels à terminaison CH_3 , CF_3 , COOR , NH_2 et OH . Les mesures de forces locales d'adhésion permettent de déterminer le travail thermodynamique d'adhésion (W_0) pointe-surface ainsi que l'énergie de surface (γ_s) de tels systèmes. Les effets de ponts capillaires doivent être pris en compte lorsqu'il y a contact hydrophile-hydrophile. Dans une troisième partie, nous montrons, par l'étude de réseaux polymères de chimie de surface contrôlée par greffage de couches fonctionnelles auto-assemblées, qu'il est possible de découpler les contributions chimique et mécanique dans le contact adhésif. Les résultats montrent que la force d'adhésion est proportionnelle à W_0 et à une fonction de dissipation locale f , proportionnelle à M_c , la masse moyenne entre nœuds de réticulation. Nous montrons que les grands principes du modèle rhéologique de l'adhésion restent pertinents à une échelle locale. **Pour citer cet article :** M. Brogly et al., C. R. Chimie 9 (2006).

© 2005 Académie des sciences. Published by Elsevier SAS. All rights reserved.

* Corresponding author.

E-mail address: maurice.brogly@uha.fr (M. Brogly).

Keywords: Adhesion; Atomic-Force Microscopy; Surface energy; Self-Assembly Monolayer; PDMS; Nanoscale

Mots-clés : Adhésion ; Microscopie à force atomique ; Énergie de surface ; Autoassemblage ; PDMS ; Échelle nanométrique

1. Introduction

The Atomic-Force Microscope (AFM) is a promising device for the investigation of materials surface properties at the nanoscale. Precise analysis of adhesive and mechanical properties, and in particular, of model polymer surfaces can be achieved with a nanometer probe. The purpose of this study is to dissociate the different contributions (chemical and mechanical) included in an AFM force-distance curve in order to establish relationships between interfacial tip-polymer interactions and surface viscoelastic properties of the polymer. Measurements of local adhesive forces between a silicon nitride tip (Si_3N_4) and model substrates are performed by using the AFM contact mode, at ambient temperature, in the air. Considering that the main technical uncertainties have been listed and minimized, surface force measurements are, in a first step, done on chemically modified silicon substrates (grafted with hydroxyl, amine, methyl and ester functional groups). In order to investigate the effects of mechanical or viscoelastic contributions, force measurements on model polymer networks, whose surfaces are chemically controlled with the same functional groups as before (silicon substrates) were achieved. The results show that the viscoelastic contribution is dominating in the adhesion force measurement. At the end of this study, new relationships are proposed between the local adhesion force and both the dissipation energy in the tip-polymer contact and the surface properties of the materials (thermodynamic work of adhesion). Moreover the dissipation function is related to M_c , the mass between crosslinks of the network.

2. The state of the art

It is important to mention recent works that have contributed to the understanding of adhesion mechanisms at a local scale. Burns and al. [1] have demonstrated the influence of adhesion on sliding and on friction forces on chemically modified surfaces. Jones and al. [2] have studied the effects of relative humidity, rough-

ness and surface treatment on adhesive properties of glass-glass contact. Rabinovich [3] has considered the influence of roughness at the nanometer scale. But none of these studies has been devoted to the contact between a local probe and a chemically modified polymer surface. The main reason is the difficulty of quantitative interpretation of the results obtained on viscoelastic materials [4,5]. However, Basire and Fretigny [6] have done important work that allow them to determine static and dynamic modulus of polymers even if the Dupre energy they found appears to be rather small (10 mJ.m^2). Nysten and Cuenot [7,8] have conducted oscillatory experiments of an AFM probe under electrostatic field. The resonant frequency of the probe is directly related to the mechanical properties of the studied material. Finally, Aimé and his team [9,10] have studied dissipative phenomena in the adhesive contact by using dynamic AFM. They propose an original model [11] for the determination of polymer viscosity on the basis of Non-Contact resonant AFM mode. Nevertheless none of these studies was done on chemically modified polymer surfaces in order to investigate the interplay between surface chemistry and mechanical properties at a local scale.

3. Materials

Si(100) silicon wafers (Mat Technology France) polished on one side were used as substrate for the adsorption of Self Assembly Monolayers (SAMs). In this paper, “as received silicon ($\text{Si}_{\text{as received}}$)” refers to a silicon wafer previously cleaned with ethanol in an ultrasonic bath. That means that a contaminated layer still remains on the surface. Four organosilane grafts (supplied by ABCR Karlsruhe-Germany) were used for the elaboration of homogeneous model surfaces on the substrate. Two hydrophobic model surfaces were prepared by using hexadecyltrichlorosilane ($\text{C}_{16}\text{H}_{42}\text{O}_3\text{Si}$ or $\text{Si}-\text{CH}_3$) and 1H,1H,2H,2H-perfluorodecylmethyl-dichlorosilane ($\text{C}_{11}\text{H}_7\text{Cl}_2\text{F}_{17}\text{Si}$ or $\text{Si}-\text{CF}_3$) and two hydrophilic model surfaces by using (6-aminohexyl)-aminopropyltrimethoxysilane ($\text{C}_{12}\text{H}_{30}\text{N}_2\text{O}_3\text{Si}$ or $\text{Si}-$

NH₂) and 2(carbomethoxy)ethyltrichlorosilane (C₄H₇Cl₃O₂Si or Si–COOR). Polymers, namely polydimethylsiloxane (PDMS) were supplied by ABCR (Karlsruhe, Germany). All other chemicals used in chemical handling (cleaning, synthesis) were of reagent grade or better (supplied by Aldrich).

3.1. Preparation of oxidized silica surface

Before coating, the substrates must be chemically modified in order to get a hydrophilic surface (SiO₂). The silicon surface is first cleaned with ethanol and dried with nitrogen before oxidation. Then, oxidized surfaces are obtained after cleaning the substrate in a warm Piranha (60 °C) solution (3:7 v/v 30% H₂O₂ and H₂SO₄ mixture) for about 30 minutes in order to keep a smooth surface, and then, thoroughly rinsed with deionized and twice distilled water. Just before being grafted with organosilane the wafers are dried with nitrogen. This treatment produces a high hydroxyl group density on the surface (SiOH groups), to which functional silanes will adsorb upon hydrolysis [12].

Silicon wafers covered with hydroxyl end-groups (Si–OH) were obtained with this method and immediately probed in order to avoid contamination of the surface by the environment due to the high reactivity of silanol groups. Typical time between the drying process and the first experiment is 10 min. Hundred measurements are done for a given surface. The time constant of an experiment is 0.1 s (10 Hz).

3.2. Grafting of functionalized SAMs on silicon wafer

Three different techniques are frequently used to obtain SAMs: Langmuir–Blodgett techniques, involving an air–water interface to transfer the assembled film to a solid substrate, solution adsorption of graft mol-

ecules onto the substrate, and vapour–phase molecular self-assembling technique [12], which uses vapour deposition of the film onto the substrate. The functionalized SAMs used in this study were prepared with the last technique slightly improved in the laboratory [13]. The lack of solvent prevents the SAMs from a possible incorporation and contamination of solvent molecules and defects. Moreover, a previous study [14] showed that the molecular films prepared with this method, are more homogeneous.

The silicon wafers are placed above a previously de-aired solution of 100 µl of organosilane - 3 ml of paraffin mixture. The vapour-phase deposition of the molecular film on the substrate is performed in a vacuum chamber (50 min at 5 × 10⁻³ Torr) at room temperature.

3.3. Cross-linking and functionalization of PDMS networks

PDMS samples were cross-linked under nitrogen in a glove box using tetrakis(dimethylsiloxy)silane as a cross-linker and a platinum-based catalyst. All the chemicals were supplied by ABCR (Karlsruhe, Germany). All the size and mechanical characteristics of the different PDMS are gathered in Table 1. Mc values represent the average molecular masses between crosslinks after crosslinking. Mc values are ranging between 0.8 kg/mol and 34 kg/mol. Then, PDMS 0.8 k is the hardest substrate, whereas 34 k refers to the softest one. Mc values were determined by swelling experiments. Flory's law of rubber elasticity [15], which represents the reciprocal tensile modulus versus Mc, the mass between crosslinks, is satisfied for the synthesized networks as reported on Fig. 1. This proves that a good control of macroscopic mechanical properties is achieved. Moreover, the Young modulus is independent of the strain rate in the range of strain rate corresponding to those used during AFM experiments (at

Table 1
Size and mechanical properties of the cross-linked PDMS

PDMS	Average mass between crosslinks Mc (g/mol)	Elasticity domain (%)	Deformation at break (%)	Young modulus (MPa)
0.8 k	800	40	196	2.24
8.5 k	8500	46	210	0.64
13 k	13000	47	250	0.30
23 k	23000	50	245	0.19
34 k	34000	52	250	0.13

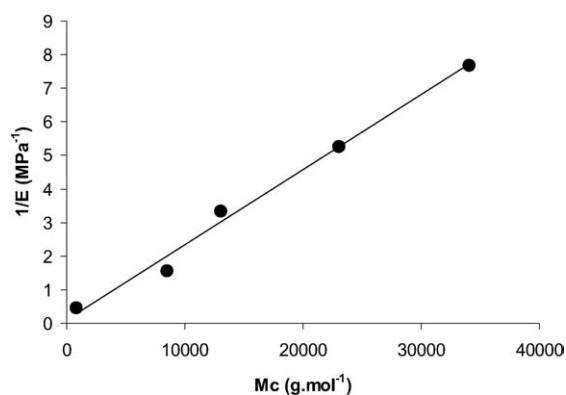


Fig. 1. $1/E = f(M_c)$ curve. E is the Young tensile modulus determined with a 1 mm/min strain rate and M_c is the average mass between crosslinks (in g/mol).

ambient temperature for all the networks). PDMS networks are then treated by water plasma and functionalization was done using the vapour deposition technique.

3.4. Characterization of the SAMs

Fig. 2 represents, as an example, AFM topographic and phase contrast images of the Si-CH₃ wafer. Tapping mode images confirm that no aggregates were formed and show a complete homogeneous recovery of the grafts. Average roughnesses are ranging between 0.1 nm (Si-OH) and 0.3 nm (Si-CH₃), whatever the grafted substrate. On PDMS substrates, average roughness is equal to 0.5 nm whatever the grafted molecules. These values confirm that the grafts are well ordered and packed at nanometer scale.

Contact angle measurements with water droplets, surface energy (determined by wettability) and ellipsometric results obtained on wafer and PDMS grafted substrates are gathered in Table 2.

Contact angle measurements (Table 2) show that grafting is effective and values obtained correspond to expected one [16]. Same comments are valid for surface energy values. Thicknesses of organic SAM films

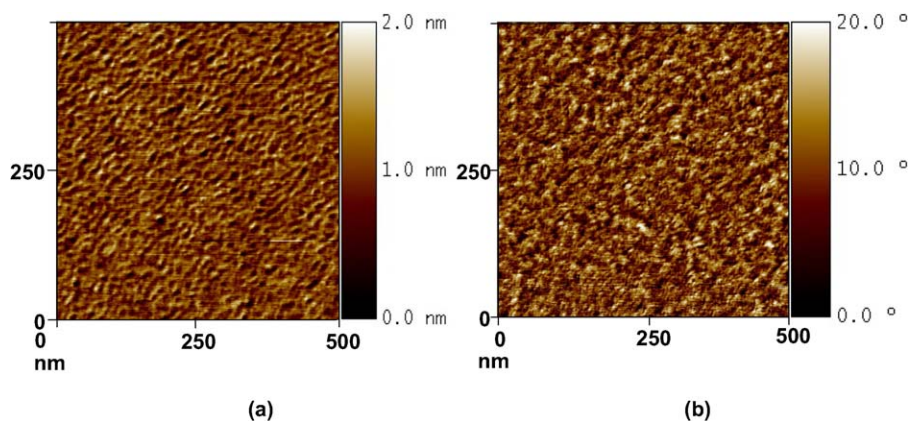


Fig. 2. Topographic (a) and phase contrast (b) images (500 nm × 500 nm) of a CH₃-grafted silicon wafer.

Table 2

Water contact angles, surfaces energies and thicknesses of SAM on silicon wafers and PDMS substrates

Substrates	Contact angle of water (°)	Surface energy (mJ/m ²)	Experimental SAM thickness (Å)	Theoretical SAM thickness (Å)
Si-CF ₃	106 ± 2	21 ± 1	12 ± 1	14
Si-CH ₃	103 ± 2	22 ± 1	21 ± 1	22.5
Si _{asreceived}	78 ± 2	32 ± 1	—	—
Si-COOR	71 ± 2	43 ± 1	5 ± 1	6
Si-NH ₂	57 ± 2	53 ± 1	9 ± 2	15
Si-OH	6 ± 2	76 ± 1	—	—
PDMS	104 ± 4	28 ± 1	—	—
PDMS-CH ₃	108 ± 4	22 ± 1	22 ± 2	22.5
PDMS-NH ₂	50 ± 4	53 ± 1	10 ± 3	15

were determined by ellipsometry (Sopra ES4 M ellipsometer) measurements by fitting the refractive index and the thickness of the organic film. Experimental values are in good agreement (Table 2) with the estimated theoretical values [17–19]. Values reported in the literature correspond to untilted grafts relative to the surface plane. In fact the graft molecules are tilted with a characteristic angle between the long-molecular axis and the surface normal [20]. This angle explains the difference between experimental and theoretical values. Nevertheless ellipsometric results confirm that only a monolayer is formed whatever the substrate and the grafted molecule.

All the AFM imaging, ellipsometric and contact angle measurements performed on the SAMs show that homogeneous and well packed grafting is obtained both on the silicon wafers and PDMS.

4. Results and discussion

4.1. Force–distance curve measurements and AFM calibration

4.1.1. Force–distance curve features

Force measurements with AFM, in the contact mode, consist in detecting the deflection of a spring (or canti-

lever) bearing a nitride silicon tip at its end, when interacting with the sample surface. The deflection of the cantilever is detected by an optical device (four quadrants of photodiodes) while the tip is vertically moved forward and backward thanks to a piezoelectric ceramic (or actuator). Thus, provided that the spring constant of the cantilever is known, one can obtain a deflection–distance (DD) curve and then a force–distance (FD) curve, by using Hooke's law. The DD curves were performed in the air with an available commercial apparatus (Nanoscope IIIa D3000, Digital Instruments). A schematic representation of a DD curve obtained when probing a hard surface is reported in Fig. 3.

4.1.2. Description of the DD curve (contact mode)

In zone A, the cantilever is far from the surface and stays in a state of equilibrium (no interaction with the surface). The cantilever deflection is zero. During the approach toward (or withdrawal from) the surface, the tip interacts with the sample and a jump in (or jump-off) contact occurs (zones B (for loading) and F (for unloading)). These instabilities take place because the cantilever becomes mechanically unstable. Usually, for underformable surfaces, because of mechanical instabilities, jump-in contact is not significant to determine, quantitatively, attractive Van der Waals forces. When in contact, the cantilever deflection is equal to the piezo-

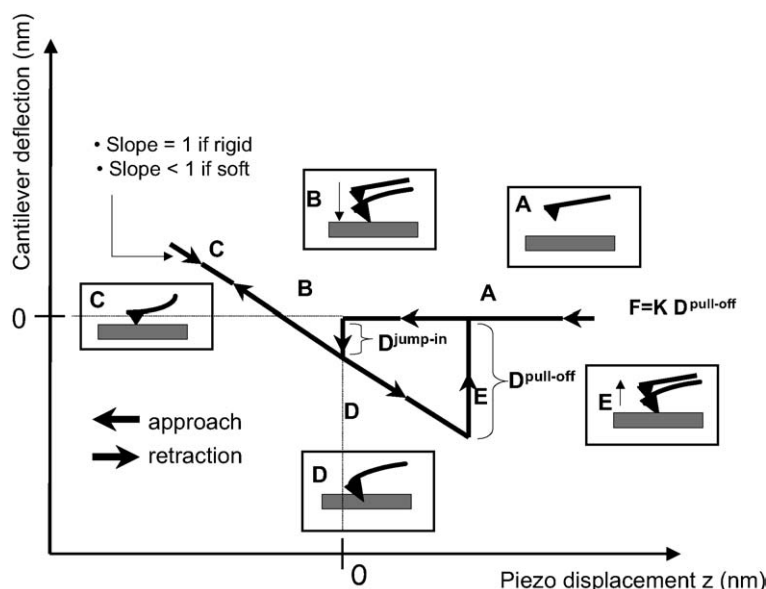


Fig. 3. Schematic representation of a DD curve. The slope of the 'contact zone' is equal to unity when considering the contact between the tip and a rigid surface, whereas it is lower than 1 when considering the contact between the tip and a soft material (polymer).

electric ceramic displacement provided no indentation of the substrate occurs (zones C (for loading) and D (for unloading)). An underformable reference sample (cleaned silicon wafer) is used to scale the DD curve in deflection by fixing to unity the slope value of the contact line.

4.1.3. AFM calibration

One of the fundamental points to obtain reproducible, quantitative and reliable data is the calibration procedure, which should be rigorous and systematic for all measurements.

4.1.3.1. Determination of the spring constant of the cantilever. To determine the spring constant of the cantilever, a non-destructive method, based on the use of reference rectangular cantilevers [21] was used. The cantilevers used in this study, were triangular shaped cantilevers (supplied by Nanosensor-Germany) and have effective spring constant equal to $0.30 \pm 0.03 \text{ N m}^{-1}$ (the value specified by the supplier is 0.58 N m^{-1}). Cantilevers having the same spring constant were chosen for this study.

4.1.3.2. Non-linearity of the quadrant of photodiodes. The non-linearity of the optical detector is the consequence of a non-homogeneous spreading of the laser spot on the detector. This non-linearity has been studied by reporting the slope of the contact line (zones C or D) of the DD curve (obtained on a hard surface and considering that there is no non-linearity at the middle of the photo detector) versus the tension (V) measured by the detector. The domain of linearity of the detector lies between $\pm 2 \text{ V}$. If non-linearity is not taken into account, the error on the quantitative results can be significant, because the slope of the contact line determines the Y -scale.

4.1.3.3. Scan rate of the cantilever. The actuator shows hysteresis in its vertical displacement. This hysteresis can be studied by reporting the slope of the contact zones (zones C and D) versus the amplitude of the contact zone and the scan rate. During the experiments, the actuator is considered as thermally stable. We observed that a discrepancy appears for very low scan rates. For higher scan rates, the viscosity of the environment could be significant. A rate of about $6 \mu\text{m}\cdot\text{s}^{-1}$ is a good compromise.

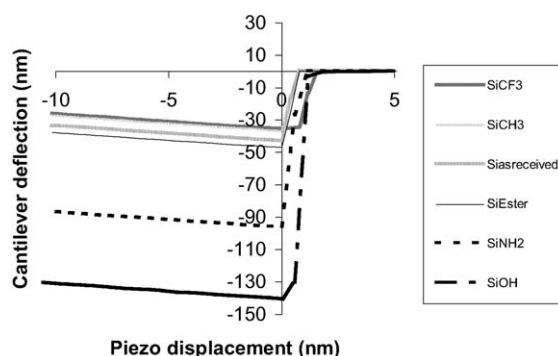


Fig. 4. Experimental DD curves (retraction) on functionalized silicon wafers.

4.1.3.4. Systematic checking. In addition, checking regularly and randomly the adhesion force on a reference silicon wafer verifies contamination of the tip during the measurements. When the tip is contaminated, a new tip is used and characterized. In that way, selected tips have the same radius and the same spring constant in order to compare the experimental values. We mention that tip contamination occurs a few in comparison of the great number of DD experiments. Finally, the reported results are an average of about 100 DD curves for each substrate. Relative uncertainty is equal to 8% in all cases [13].

4.2. Force–distance curves on rigid systems of controlled surface chemistry

The tip-sample pull-off force was first measured on chemically modified SAMs obtained on undeformable substrates (silicon wafers) and was compared with that for as received silicon wafer. Fig. 4 shows that AFM measurements in our conditions are sensitive to a chemical modification of the wafer surface by adsorption of SAM. When jump-off (or jump-in) contact occurs, the corresponding pull-off deflection (or pull-in) is measured. Pull-off deflection values ($D^{\text{pull-off}}$) increase in the following order:

$$D^{\text{pull-off}}_{\text{SiCF}_3} < D^{\text{pull-off}}_{\text{SiCH}_3} < D^{\text{pull-off}}_{\text{Si as received}} < D^{\text{pull-off}}_{\text{SiCOOR}} < D^{\text{pull-off}}_{\text{SiNH}_2} < D^{\text{pull-off}}_{\text{SiOH}}$$

Knowing the pull-off deflection one can easily deduce the adhesion force, knowing the cantilever spring constant k :

$$F_{\text{adh}} = kD^{\text{pull-off}} \quad (1)$$

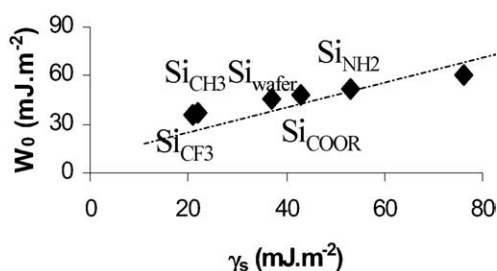


Fig. 5. Thermodynamic work of adhesion deduced from AFM (DMT theory) versus surface energy of SAMs grafted wafers.

k has been determined according to the method described in [21]. The pull-off deflection and thus the adhesion force value increases with the hydrophilicity of the surface. The measured adhesion force depends strongly on the tip radius in the case of undeformable substrates. Sugawara and al. [22] suggested that the adhesion force is proportional to the tip radius.

The DMT theory [23], also establish a relationship between the adhesion force (F), the tip radius (R) and the thermodynamic work of adhesion (W_0):

$$F_{\text{adh}} = 2 \pi R W_0 \quad (2)$$

On the basis of this relation one can deduce W_0 from experimental adhesion forces. Fig. 5 shows that the thermodynamic work of adhesion, W_0 , is proportional to the surface energy deduced from classical wettability measurements.

In the case of hydrophilic surfaces (Si–NH₂, Si–OH), the AFM tip interacts with the water layer adsorbed on the surface and the measured adhesion force results from the adhesion between water adsorbed on the both surfaces (tip and sample) and from the adhesion force due to the Van der Waal force between the NH₂ or OH sites existing at the grafted wafer surface. On the contrary, during wettability experiments the water droplet deposited on the surface does not feel the OH sites existing at the hydroxylated wafer surface.

For technical reasons, all the AFM measurements were done in the air at about 20 °C. Under these conditions, the influence of the capillary forces cannot be neglected. Indeed, all the experiments were done at a constant relative humidity of 30%. Many studies have reported the effect of humidity on the separation force. Xiao and al. [24] and Sedin and al. [25] have shown that a water meniscus cannot be formed between the tip and the surface if relative humidity is below 20%. He and co-workers [26] have observed a meniscus for-

mation only in the case of hydrophilic contact but not for hydrophobic contact. These results are confirmed by Zhong and al. [27]. Salmeron [28], for an hydrophilic tip-Mica contact has observed that water capillary effects are significant if relative humidity is higher than 40%. As in our experiments the humidity is of 30% one can suspect the existence of a capillary bridge. On the theoretical point of view, the minimum thickness of the water capillary film is expressed as [29,30]:

$$e = a_0 \left(\frac{\gamma_w}{S} \right) \quad (3)$$

Where e is the film thickness, γ_w the surface tension of water, a_0 a capillary length and S the spreading coefficient ($S = \gamma_s - \gamma_{\text{SL}} - \gamma_L$).

As a consequence, the force measured by AFM includes the contribution of Van Der Waals and capillary forces. The total adhesion force is given by the following expression:

$$F_{\text{adh}} = F_{\text{cap}} + F_{\text{VDW}} \quad (4)$$

The capillary force depends on a meniscus formed between the two surfaces and is given by Israelachvili [16] and by Riedo and al. [31], in the case of sphere-plane contact, by:

$$F_{\text{cap}} = 2 \pi R \gamma_w (\cos\theta_{\text{w/tip}} + \cos\theta_{\text{w/wafer}}) \quad (5)$$

where γ_w is the surface tension of water, R the tip radius and θ the contact angle between water and the tip (determined on the back side of the cantilever) or water and the wafer. In a recent study, Weeks and al. [32] have used environmental scanning electron microscopy to image water meniscus formation between an AFM tip and a surface.

Values of W_0 (Fig. 5) were obtained after correction from capillary forces effects on Si–NH₂ and Si–OH hydrophilic surfaces.

4.3. The specific case of force–distance measurements on polymers

A comparison between the DD curves obtained on a silicon substrate and on a PDMS substrate shows important differences probably due to the specific mechanical behavior of PDMS polymer chains (Fig. 6). First compared to silicon wafer, in the tip-polymer separation process, the jump-off contact occurs over a large

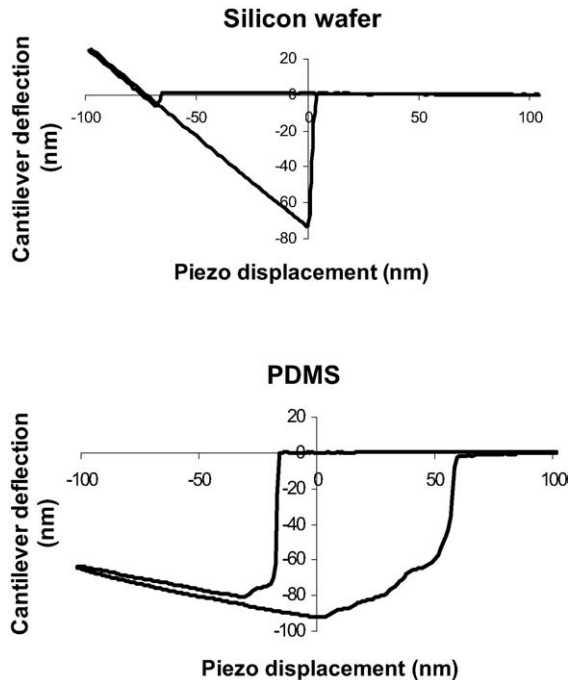


Fig. 6. Comparison between a DD curve obtained on a silicon substrate (top) and a PDMS substrate (bottom).

piezo displacement scale and could correspond to a progressive dewetting of the tip by polymer chains during tip retraction. Second, the jump-off amplitude is higher than for silicon wafer. Finally, the loading and unloading slope in the DD representation is much lower than unity in the case of soft polymer systems. The beginning of the indentation is assumed to be at the minimum of the DD curve. Creep experiments have also been performed with the AFM. Considering the experimental contact time ($t_{\text{exp}} < 0.1$ s), the creep effect is neglected in our force curve measurements (Fig. 7).

Nevertheless a crucial question concerns the beginning of indentation in the specific case of soft poly-

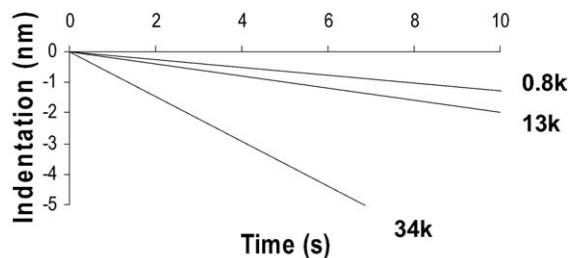


Fig. 7. Creep experiments (Indentation (nm) vs time (s)) with the AFM (corrected from thermal drift) on the 0.8-k, 13-k and 34-k PDMS networks.

mers. Indeed, for very low modulus materials, the jump-in contact deflection appears to be very important and somehow comparable to the jump-off contact (Fig. 6). Such an amplitude (60–80 nm) could not be only due to mechanical instability of the cantilever, estimated to be equal to 4–5 nm. In order to explain the important deflection when contact occurs, we propose the hypothesis of the formation of a nanoprotuberance at the PDMS surface. This protuberance comes into contact with the AFM tip and relaxes till zero deformation of the surface. This relaxation induce a high deflexion of the tip. Aime and al. [33] have proposed such a model that takes into account the polymer viscoelasticity. As our PDMS present very low modulus and high elasticity we have used and adapted a model based on linear elasticity [34]. Detailed information could be find in [13]. Briefly, at a given time t , the AFM tip is at a distance $d(t)$ from the polymer surface. The tip-surface interaction force is $F(t)$. This force produces the formation of a nanoprotuberance of height $h(t)$. At time $t + \Delta t$, the tip-sample distance is:

$$d(t + \Delta t) = d(t) - h(t) - p(\Delta t) - \delta(t) \quad (6)$$

where $p(\Delta t)$ is the piezo displacement and $\delta(t)$ is the cantilever deflection. Then on, the force $F(t + \Delta t)$ and height are calculated. Fig. 8 gives the results of the calculation. These results show that the deflection of the cantilever is negligible when contact occurs. As a consequence, the jump-in amplitude at the approach is due to the relaxation of the nanoprotuberance till zero deformation. Due to adhesion forces, the AFM tip is pulled down in the relaxation process. Table 3 gathers the protuberance heights obtained by simulation and the experimental one. Good agreement is observed and indicates that real indentation of the polymer surface occurs at the minimum of the jump-in curve.

4.3.1. Force-indentation measurements on polymers

Before monitoring DD curves on PDMS, the actuator and the cantilever were thermally stabilized. The laser spot position on the tip was also optimized. Indeed, Warmack and al. [35] have studied the effect of the laser beam position on the cantilever when the tip is subject to tangential forces. They show that, depending on the beam position, the contribution of the tangential forces is more or less important on the detected signal. The laser spot in contact with the tip was positioned in such a way that the effect of tangential forces were mini-

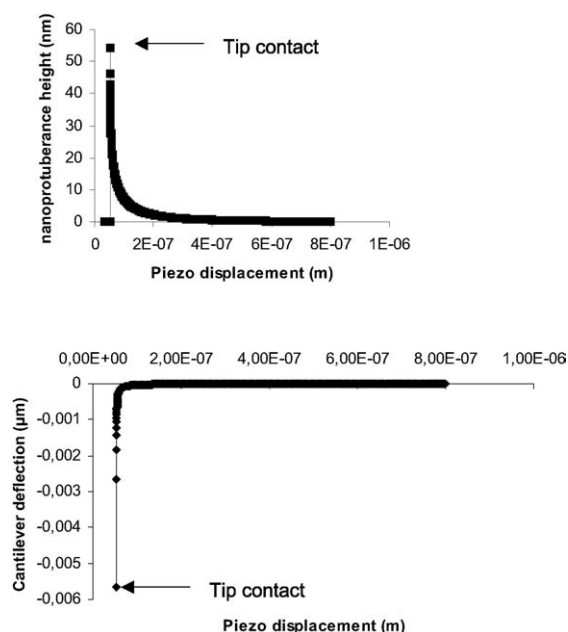


Fig. 8. Simulation of nanoprotuberance height (top) and cantilever deflection (bottom) vs piezo displacement, at the beginning of the contact.

Table 3

Nanoprotuberance heights (nm) obtained by simulation and jump-in contact amplitude (nm)

PDMS	Nanoprotuberance height (simulation) (nm)	Jump-in contact amplitude (average over 100 DD curves) (nm)
0.8 k	24	20–25
13k	50	50–65
34 k	73	70–85

mized. DD measurements were carried out on the basis of the above prerequisites so that force measurements could be liable and compared.

To deduce work of adhesion from our experimental values, it is necessary to have a good estimation of the radius of the tip. The MEB picture (Fig. 9) reveals that the tip shape can be represented as a pyramid ended by a sphere. Average tip radius of the selected tips is estimated to be equal to 50 nm \pm 5 nm on the basis of MEB pictures.

One had to ask now if the the cantilever is stiff enough to penetrate the PDMS networks. Considering the normal stiffness of the cantilever, it is possible to determine the maximum indentation depth (δ_{\max}), using the following relationship.

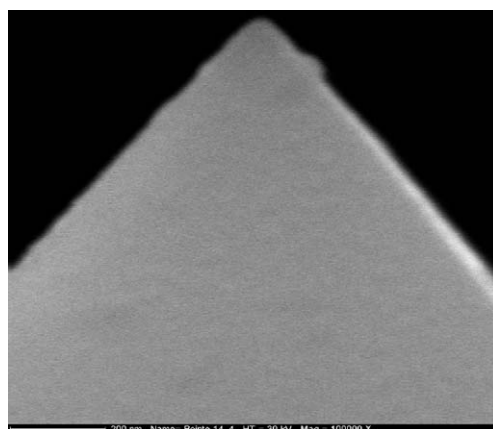


Fig. 9. MEB photography of an AFM tip.

$$k = 2 \times E^* \times \sqrt{R \delta_{\max}} \quad (7)$$

where k is the spring constant of the cantilever, E^* is the reduced modulus and R is the tip radius. δ_{\max} represents the maximum penetration depth of the tip in a given PDMS sample. Once this indentation is obtained, even if the loading of the tip is increased, the tip does not penetrate deeper in the sample. Calculation of δ_{\max} gives values ranging between 89 nm and 27 μm respectively for the hardest (0.8-k) and the softest (34-k) PDMS. In order to perform experiments at constant indentation for all the PDMS and considering that for our substrates the minimum value of δ_{\max} is 89 nm, we have decided to perform constant nanoindentation experiments up to 80 nm.

4.4. Force-indentation curves on systems of controlled surface chemistry and controlled mechanical properties

Force-indentation (F – I) curves (Fig. 10) are deduced from DD curves by assuming that for a given force, the indentation depth is the difference between the experimental deflection value (d_{soft}) and the one that should be observed if the material was underformable (d_{rigid}) deduced from the slope of 1 for underformable materials. All F – I curves obtained on PDMS and grafted PDMS have been performed at a 80-nm indentation depth, as discussed previously. We consider PDMS of different Young modulus grafted with identical molecules than silicon wafers (CH_3 and NH_2 SAMs). Fig. 10 clearly shows the influence of the network mechanical properties on F – I response when surface

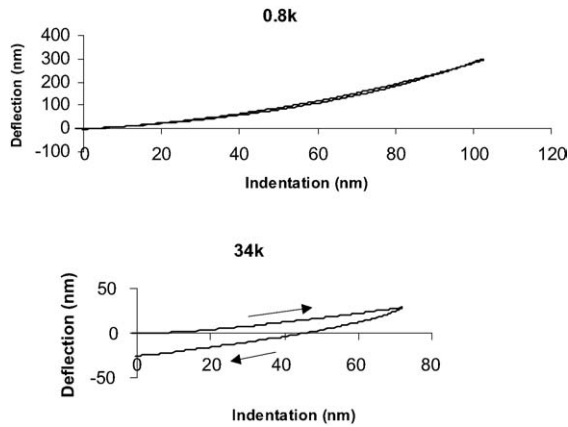


Fig. 10. Deflection vs indentation curves for PDMS 0.8 k (top) and 34 k (bottom) samples.

chemistry is constant (CH_3 grafts). For low M_c value (0.8 k), loading and unloading are quite similar and rather no dissipation of energy is observed. On the contrary, when M_c increases (34 k) unloading is greatly different from loading and dissipation and adhesive contact occur.

The following ratios $\left(\frac{F_{\text{adhPDMSX}}}{F_{\text{adhSiX}}}\right)$ (where F_{adhPDMS} and F_{adhSi} represents the adhesion (or pull-off) force measured on respectively PDMS and silicon substrates and X represents the functionality of the grafting) were calculated for all the grafting and PDMS substrates (Table 4) and compared.

It appears that for a given PDMS substrate (for example, 0.8 k), the ratios do not depend on the surface chemistry, whereas for a given grafting, the ratios depend on the mechanical properties of the substrate, having the same value for all the grafts. Thus, for a given substrate:

$$F_{\text{adhPDMSX}} = F_{\text{adhSiX}} \times C_1 \quad (C_1 \text{ is a constant}) \quad (8)$$

Table 4

Ratio $\left(\frac{F_{\text{adhPDMSX}}}{F_{\text{adhSiX}}}\right)$ for CH_3 , NH_2 and ungrafted substrates and for three PDMS of different mechanical properties

PDMS	$F_{\text{PDMS}}/$ F_{Si} ratio	$F_{\text{PDMS-CH}_3}/$ $F_{\text{Si-CH}_3}$ ratio	$F_{\text{PDMS-NH}_2}/$ $F_{\text{Si-NH}_2}$ ratio
0.8 k	1.1 ± 0.1	1.0 ± 0.1	1.2 ± 0.1
13 k	1.8 ± 0.1	1.5 ± 0.1	1.5 ± 0.1
34 k	2.0 ± 0.1	1.9 ± 0.1	2.6 ± 0.1

However, for an undeformable substrate, the DMT theory [23] gives:

$$F_{\text{adhSiX}} = 2 \pi R W_0 \quad (9)$$

Then,

$$F_{\text{adhPDMSX}} = 2 \pi R W_0 C_1 \quad (10)$$

and when introducing a dimensional constant ($C_2 = (2 \pi R)^{-1}$) this relationship becomes:

$$G_{\text{adhPDMSX}} = W_0 C_1 2 \pi R C_2 \quad (11)$$

or

$$G_{\text{adhPDMSX}} = W_0 f(M_c, \nu, T) \quad (12)$$

where G is the separation energy and $f(M_c, \nu, T)$ is a dissipative viscoelastic function that depends on the network molecular structure (M_c), temperature T , and separation rate ν .

This relationship clearly expresses the respective part of the mechanical contribution from the chemical one in a force-indentation measurement with AFM. As C_2 is a dimensional constant equal to $(2 \pi R)^{-1}$, from eqs. (11) and (12) we propose that:

$$f(M_c, \nu, T) = \{C_1\} \quad (13)$$

where $\{C_1\}$ is the average of the values of C_1 obtained for PDMS, PDMS- CH_3 and PDMS- NH_2 , and thus for a given M_c (mass between crosslinks). According to eq. (13), $f(M_c, \nu, T)$ is determined for each substrate for a given rate ($6 \mu\text{m s}^{-1}$) and a given temperature (293 K). $f(M_c, \nu, T)$ does not depend on the surface chemistry. $f(M_c, \nu, T)$ cannot theoretically be lower than 1 (which corresponds to a zero separation rate) and should increase, while the Young modulus decreases (which means energy dissipation in the bulk is higher when the network is softer). The values of $f(M_c, \nu, T)$ obtained are gathered in Table 5. Values obtained are coherent with the preceding assumptions. Moreover, even if the dependance of $f(M_c, \nu, T)$ on the separation rate ν is not dominating in the range of the available separation rates with the AFM, it is obvious (Fig. 10), that dissipation occurs for the 34-k sample and that this dissipation is included in the function f . The dissipative function f is constant for a given grafting and increases as M_c does i.e. as PDMS Young modulus decreases.

Table 5

Average viscoelastic dissipation function (f) and calculated thermodynamic work of adhesion (W_0)

PDMS	Dissipation function f	Work of adhesion W_0 (CH ₃ grafts) (mJ/m ²)	Work of adhesion W_0 (NH ₂ grafts) (mJ/m ²)
0.8 k	1.1 ± 0.1	35 ± 4	107 ± 15
13 k	1.6 ± 0.2	36 ± 4	105 ± 15
34 k	2.2 ± 0.4	32 ± 4	106 ± 15

This is an expected result, as viscoelastic dissipation should increase when the network becomes softer.

Assuming that the separation of the tip from the polymer sample could be described as a JKR process, it is also possible to determine W_0 , the thermodynamic work of adhesion. According to JKR formalism [36]:

$$W_0(X) = (2 F_{\text{adhPDMSX}}) / (3\pi R) \quad (14)$$

where $W_0(X)$ is the tip-PDMS thermodynamic work of adhesion for a given graft (X). Values of W_0 are gathered in Table 5, for each PDMS (0.8 k, 13 k, and 34 k) and for each grafting. Values of W_0 are in agreement with values obtained on silicon wafers (Fig. 5) that have the same surface chemistry and also with quoted values in the literature. Indeed, usual work of adhesion values lie between 40 to 70 mJ m⁻² for organic–organic contacts as between two silylated silica [37] and between 40 to 145 mJ m⁻² for a contact between a raw material as silica and a silylated silica. Finally we have reported in Fig. 11 the evolution of the dissipative function f versus M_c , the mass between crosslinks. A linear relationship is obtained. Therefore a modified expression of G , the separation energy is proposed:

$$f(M_c, v, T) = 1 M_c \times f'(v, T) \quad (15)$$

thus:

$$G_{\text{adhPDMSX}} = W_0 \times (1 + M_c \times f'(v, T)) \quad (16)$$

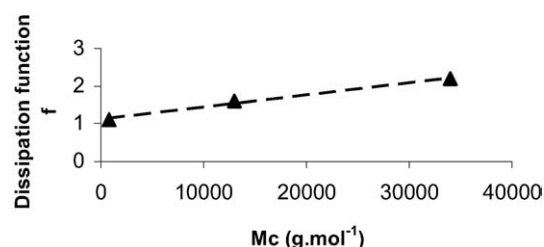


Fig. 11. Dissipation function f versus M_c , the average mass between crosslinks.

where $f'(v, T)$ represents a dissipative viscoelastic function, which depends only on the temperature T and separation rate v .

5. Conclusions

The studied model systems allowed us to express the mechanical and chemical surface contributions in a force curve measurement and to establish a relationship, which is quite similar to the relationship of Gent and Schultz [38] at the nanoscale. From then on, a new relationship is proposed to determine thermodynamic surface properties of viscoelastic materials on the basis of AFM experiments.

References

- [1] A.R. Burns, J.E. Houston, R.W. Carpick, T.A. Michalske, *Langmuir* 15 (1999) 2922.
- [2] R. Jones, H.M. Pollock, J.A.S. Cleaver, C.S. Hodges, *Langmuir* 18 (2002) 8045.
- [3] Y.I. Rabinovich, J. Adler, A. Ata, R.K. Singh, B.M. Moudgil, *J. Colloid Interface Sci.* 232 (2000) 10.
- [4] C. Basire, C. Fretigny, *Tribol. Lett.* 10 (2001) 189.
- [5] W.N. Unertl, *J. Adhes.* 74 (2000) 195.
- [6] C. Basire, PhD thesis, Université Paris-6, France, 1998.
- [7] S. Cuenot, A.S. Duwez, P. Martin, B. Nysten, *Chimie nouvelle* 79 (2002) 89.
- [8] S. Cuenot, PhD thesis, Université catholique de Louvain, Belgium, 2003.
- [9] J.-P. Aimé, R. Boisgard, L. Nony, G. Couturier, *J. Chem. Phys.* 114 (11) (2001) 4945.
- [10] R. Boisgard, J.-P. Aimé, G. Couturier, *Surf. Sci.* 511 (2002) 171.
- [11] F. Dubourg, PhD thesis, Université Bordeaux-1, France, 2002.
- [12] M.K. Chaudhury, G.M. Whitesides, *Science* 255 (1992) 1230.
- [13] O. Noel, PhD thesis, Université de haute Alsace, Mulhouse, France, 2003.
- [14] L. Vonna, PhD thesis, Université de haute Alsace, Mulhouse, France, 1999.
- [15] P.J. Flory, *Chem. Rev.* 35 (1944) 51.
- [16] J.N. Israelachvili, *Intermolecular and Surface Forces*, 2nd Edition, Academic Press, London, 1991.

- [17] J. Ruhe, V.J. Novotny, K.K. Kanazawa, T. Clarke, G.B. Street, *Langmuir* 9 (1993) 2383.
- [18] S.R. Wasserman, G.M. Whitesides, I.M. Tidswell, B.M. Ocko, P.S. Pershan, J.D. Axe, *J. Am. Chem. Soc.* 111 (1989) 5852.
- [19] M.D. Porter, T.B. Bright, D.L. Alara, C.E.D. Chidsey, *J. Am. Chem. Soc.* 109 (1987) 3559.
- [20] D.L. Allara, A.N. Parikh, F. Rondelez, *Langmuir* 11 (1995) 2357.
- [21] A. Torii, M. Sasaki, K. Hane, S. Okuma, *Meas. Sci. Technol.* 7 (1996) 179.
- [22] Y. Sugawara, M. Ohta, T. Konishi, S. Morita, M. Suzuki, Y. Enomoto, *Wear* 168 (1993) 13.
- [23] B.V. Derjaguin, V.M. Muller, Y.P. Toporov, *J. Colloid Interface Sci.* 53 (1975) 314.
- [24] X. Xiao, L. Oian, *Langmuir* 16 (2000) 8153.
- [25] D.L. Sedin, K.L. Rowlen, *Anal. Chem.* 72 (2000) 2183.
- [26] M. He, A. Szuchmacher Blum, D.E. Aston, C. Buenviaje, R.M. Overney, R. Luginbuhl, *J. Chem. Phys.* 114 (2001) 1355.
- [27] L. Zhang, L. Li, S. Chan, S. Jiang, *Langmuir* 18 (2002) 5448.
- [28] J. Hu, X.D. Xiao, D.F. Ogletree, M. Salmeron, *Surf. Sci.* 344 (1995) 221.
- [29] R. Bruinsma, *Macromolecules* 23 (1990) 276.
- [30] P.-G. de Gennes, *Rev. Mod. Phys.* 57 (1985) 827.
- [31] E. Riedo, F. Levy, H. Brune, *Phys. Rev. Lett.* 88 (2002) 185505.
- [32] B.L. Weeks, M.W. Vaughn, J.J. DeYoreo, *Langmuir* 21 (2005) 8096.
- [33] J.-P. Aimé, D. Michel, R. Boisgard, L. Nony, *Phys. Rev. B Condens. Matter* 59 (1999) 2407.
- [34] J.B. Pethica, A.P. Sutton, *J. Vac. Sci. Technol. A* 6 (1988) 2490.
- [35] R.J. Warmack, X.Y. Zheng, T. Thundat, D.P. Allison, *Rev. Scientific Instr.* 65 (1994) 394.
- [36] K.L. Johnson, K. Kendall, A.D. Roberts, *Proc. R. Soc. A* 324 (1971) 301.
- [37] E. Papirer, H. Balard, M. Sidqi, *J. Colloid Interface Sci.* 159 (1993) 238–242.
- [38] A. Gent, J. Shultz, *J. Adhes.* 3 (1972) 281.